Neuron, Vol. 18, 473–481, March, 1997, Copyright ©1997 by Cell Press

Low Mobility of the Ca^{2+} Buffers in Axons of Cultured Aplysia Neurons

Moshe Gabso,* Erwin Neher,† and Micha E. Spira*
*Department of Neurobiology
Life Sciences Institute
The Hebrew University of Jerusalem
The Interuniversity Institute for Marine Sciences of Eilat
Israel
†Max-Planck-Institut fuer Biophysikalische Chemie
D-37033 Goettingen
Federal Republic of Germany

Summary

Cellular Ca^{2+} buffers determine amplitude and diffusional spread of neuronal Ca^{2+} signals. Fixed Ca^{2+} buffers tend to retard the signal and to lower the apparent diffusion coefficient (D_{app}) of Ca^{2+}, whereas mobile buffers contribute to Ca^{2+} redistribution. To estimate the impact of the expression of specific Ca^{2+}-binding proteins or the errors in Ca^{2+} measurement introduced by indicator dyes, the diffusion coefficient D_e and the Ca^{2+}-binding ratio κ_e of endogenous Ca^{2+} buffers must be known. In this study, we obtain upper bounds to these quantities ($D_e < 16\ \mu m^2/s$; $\kappa_e < 60$) for axoplasm of metacerebral cells of Aplysia california. Due to these very low values, even minute concentrations of indicator dyes will interfere with the spatiotemporal pattern of Ca^{2+} signals and will conceal changes in the expression of specific Ca^{2+}-binding proteins, which in the native neuron are expected to have significant effects on Ca^{2+} signals.

Introduction

A large number of cellular functions are controlled by the intracellular concentration of calcium (Miller, 1991). Yet, under normal physiological conditions, only a fraction of possible Ca^{2+}-dependent processes are activated in response to a transient elevation of the free intracellular calcium concentration ($[Ca^{2+}]_i$) caused by a given set of stimuli. It is presumed that the activation of one specific Ca^{2+}-dependent process out of many is possible since at least three aspects are relevant to activate each single process. These are: (I) The affinity to Ca^{2+} may differ for different processes. Thus, for any given "window" of $[Ca^{2+}]_i$, a subset of processes is activated. (II) The on rate of different processes may vary. As a result, the Ca^{2+}-dependent processes that are activated are defined by the duration to which the Ca^{2+} signal is present, and (III) the Ca^{2+}-dependent target molecules may be unevenly distributed in the cytosol. Thus, the location of the activated calcium source and the range of Ca^{2+} diffusion restricts the volume of cytosol that can be influenced by the Ca^{2+} signal (for example, Jaffe et al., 1992; Fields and Nelson, 1994; Spruston et al., 1995). In the present study, we focus on the analysis of some of the parameters that determine the range of calcium action in neurons.

The range of Ca^{2+} action is determined by two processes: Ca^{2+} diffusion and Ca^{2+} removal. Ca^{2+} removal is handled by either sequestration to organelles or by transport across the plasma membrane, whereas Ca^{2+} diffusion is mainly determined by the Ca^{2+} buffers. For example, after entering through voltage-gated channels, >95% of the Ca^{2+} ions bind to chelators or other binding sites located within a distance of 10–50 nm from the site of entry (reviewed by Neher, 1995). Further, Ca^{2+} diffusion is mainly determined by whether those Ca^{2+}-binding sites are fixed or mobile. Fixed binding sites, which may be located on cellular organelles or cytoskeletal elements, retard Ca^{2+} diffusion. Mobile binding sites, such as soluble Ca^{2+}-binding proteins or small molecules involved in metabolism, such as ATP and GTP, act to enhance Ca^{2+} diffusion and to enlarge the range of Ca^{2+} action. Their action is very potent, even if they diffuse at a slower rate than the free Ca^{2+} ion, due to their competition with fixed Ca^{2+}-binding sites (Zhou and Neher, 1993).

Unfortunately, it is very difficult to separate experimentally the various processes contributing to Ca^{2+} redistribution, and it seems that to date no experimental data are available that would allow us to estimate the contribution of fixed buffers, mobile buffers, and extrusion mechanisms separately under in vivo conditions.

Hodgkin and Keynes (1957) already recognized that diffusion of radioactivity-labeled Ca^{2+} was retarded in the squid giant axon. They determined the 'retardation factor' to be about 40. However, the radioactive tracer measurement was performed on the minute timescale and over millimeter distances–a regime in which equilibration with Ca^{2+}-sequestering organelles occurs, such that only the combined effect of the buffering and sequestration processes was assayed. Poisoning of the Ca^{2+}-sequestration processes allowed a more detailed investigation of the contributions of these mechanisms. More recently, Allbritton et al. (1992) performed a very careful study on cytosolic extracts of Xenopus oocytes. They obtained cytoplasm, blocked metabolism and Ca^{2+}-transport mechanisms, and determined the apparent diffusion coefficient (D_{app}) of both Ca^{2+} and IP_3. They found that D_{app} for Ca^{2+} at low free $[Ca^{2+}]$ was 13 $\mu m^2/s$, much lower than that of IP_3, which was 283 $\mu m^2/s$. The low value of D_{app} for Ca^{2+} increased when the free $[Ca^{2+}]$ was increased, in accordance with the idea that at higher $[Ca^{2+}]$, some of the fixed buffers are saturated and therefore can no longer retard diffusion. This work, recent studies by Al-Baldawi and Abercrombie (1995a) on extracted axoplasm from Myxicola, and a number of recent theoretical studies (Sala and Hernandez-Cruz, 1990; Nowycky and Pinter, 1993) clearly demonstrate the important effects of fixed Ca^{2+} buffers on Ca^{2+} diffusion.

An open question, however, is whether in vivo there are additional mobile buffers, which are lost during handling of the cytoplasmic samples or by 'washout' in a whole-cell patch-clamp situation. Simple estimates about the mutually competing effects of fixed and mobile buffers show that the presence of reasonable amounts of ATP alone may by itself speed up diffusion

of Ca^{2+} by a factor of 2 to 3 above the 'floor value' prevailing in the case that only fixed buffers are present (Zhou and Neher, 1993). Many cell types in the central nervous system are known to express specific Ca^{2+}-binding proteins (reviewed by Heizmann and Braun, 1995), and it is important to know how these may influence their functions.

Another crucial question related to the study of calcium dynamics in neurons is at what concentration and to what extent does an exogenous Ca^{2+} indicator, such as fura-2, affect the spatiotemporal distribution pattern of the intracellular Ca^{2+}?

In this study, we attempted to determine the apparent Ca^{2+} diffusion coefficient (D_{app}) in intact cylindrical axons of identifiable cultured Aplysia neurons in situ. This was done by analyzing Ca^{2+} redistribution after its local intracellular microinjection. We performed these experiments under conditions in which the mobile Ca^{2+} buffers could not be washed away, and at a range of fura-2 concentrations that allowed us to extrapolate to zero [fura-2]. Our study clearly shows that the buffering background of axoplasm in the metacerebral neurons of Aplysia is low, both in its Ca-binding ratio (ratio of bound over free Ca^{2+}) and in its mobility. Being a mobile Ca^{2+} chelator, fura-2 strongly influences Ca^{2+} redistribution at concentrations that are commonly used in imaging studies. Due to the low background in buffering, expression of specific Ca^{2+}-binding proteins will have pronounced affects on Ca^{2+}-signaling, which, however, will hardly show up in Ca^{2+}-imaging experiments due to the perturbation induced by indicator dyes.

Results and Discussion

Theory

In Aplysia neurons, Ca^{2+} removal following Ca^{2+} influx is a relatively slow process. When $[Ca^{2+}]$ is elevated uniformly by a train of action potentials, typical time constants of Ca^{2+} decay observed throughout a cylindrical axonal process are in the range 3–10 s (Gabso et al., 1996, unpublished data). Binding to Ca^{2+}-binding proteins and chelators, on the other hand, typically occurs on the microsecond to millisecond time scale (Falke et al., 1994). Thus, the processes of Ca^{2+} removal and Ca^{2+} buffering are well separated kinetically. The time resolution of Ca^{2+} imaging can resolve the slow removal process but, in general, not the fast Ca^{2+}-buffering reactions.

A Ca^{2+} transport equation for this situation was developed by Wagner and Keizer (1994), which assumes several buffer species, both mobile and fixed to be at local equilibrium with the free $[Ca^{2+}]_i$ and to contribute (if mobile) to Ca^{2+} transport. For the case that diffusion coefficients of Ca^{2+}-bound and free forms of buffers are equal and that maximum Ca^{2+} elevations are sufficiently small, i.e., $[Ca^{2+}]_i$ is smaller than the dissociation constants of mobile buffers, the transport equation takes the simple form of the classical diffusion equation with an apparent diffusion constant D_{app} (equations 44–46 of Wagner and Keizer, 1994):

$$D_{app} = (D_{Ca} + \sum_i D_{m,i}\kappa_{m,i})/(1 + \sum_i \kappa_{m,i} + \sum_j \kappa_{s,j}) \quad (1)$$

Here, the nomenclature of Zhou and Neher (1993) is used with indexes m and s representing mobile and fixed buffer species, D_{Ca} the diffusion coefficient of free calcium, D_m that of mobile Ca^{2+} buffers, and κ_m and κ_s the Ca^{2+}-binding ratios (ratio of bound to free Ca^{2+}) for mobile and fixed buffers, respectively. The latter are given by

$$\kappa_m = \frac{[B_m]_T K_m}{(K_m + [Ca^{2+}])^2} \quad (2)$$

where $[B_m]_T$ and K_m are the total concentration and Ca^{2+} dissociation constant of the respective buffer and $[Ca^{2+}]$ is the steady state calcium concentration. As mentioned above, the theory is valid only for small $[Ca^{2+}]$ values for which $[Ca^{2+}] << K_m$, such that

$$\kappa_m \approx [B_m]_T / K_m \quad (3)$$

Ca^{2+} diffusion in a cylinder was considered by Zador and Koch (1994). They showed that under simplifying assumptions, as outlined above, a perfect analogy holds between diffusion and the classical cable equation for electrical conduction in a leaky cable. In this analysis, only longitudinal diffusion is considered or else Ca^{2+} and buffers are assumed to have reached equilibrium in the radial direction. The Ca^{2+} extrusion mechanisms are lumped into a linear pump term. Their equation (13), using the notation above, can be written

$$\frac{\delta[Ca^{2+}](x,t)}{\delta t} = D_{app}\frac{\delta^2[Ca](x,t)}{\delta x^2} - \frac{2 \cdot \{P_m[Ca^{2+}](x,t) - K_\infty I(x,t)\}}{a \cdot (1 + \sum_i \kappa_{m,i} + \sum_j \kappa_{s,j})} \quad (4)$$

Here, the product $P_m[Ca^{2+}](x,t)$ represents the Ca^{2+} extrusion in mol/(cm²s); $K_\infty I(x,t)$ represents the Ca^{2+} load by a Ca^{2+} current I(x,t) and 2/a is the surface to volume ratio of a cylinder with radius a.

During most of this work, we consider a short Ca^{2+} injection at x = 0 and unpertubed Ca^{2+} diffusion thereafter. Following the injection I(x,t) will be constant and negligible. We will look for a solution of the form

$$[Ca^{2+}](x,t) = y(x,t)\exp(-t/\tau) + [Ca^{2+}]_\infty \quad (5)$$

Inserting this into equation (4), we find that y(x,t) follows the simple diffusion equation

$$\frac{\delta y(x,t)}{\delta t} = D_{app}\frac{\delta^2 y(x,t)}{\delta x^2} \quad (6)$$

when

$$\tau = \frac{a}{2P_m}(1 + \sum_i \kappa_{m,i} + \sum_i \kappa_{s,i}) \quad (7)$$

In response to a short perturbation, equation (6) has the well known solution

$$y(x,t) = A_0 \frac{\exp(-x^2/(4D_{app}t))}{\sqrt{4\pi D_{app}t}} \quad (8)$$

with A_0 depending on the strength of the injection. If the cylindrical structure is long compared to diffusional distances during an experiment, we can integrate the Ca^{2+} deflection from baseline over the whole cylinder and obtain

$$\int_{-\infty}^{+\infty} \{[Ca^{2+}](x,t) - [Ca]_\infty\}dx = \exp(-t/\tau) \int_{-\infty}^{+\infty} y(x,t)dx$$
$$= A_0 \exp(-t/\tau) \quad (9)$$

This shows that the spatial integral plotted as a function of time should readily give a time constant, according to equation (7), which reflects the Ca^{2+} retrieval rate and the total Ca^{2+} buffer capacity of the axon.

Analysis of the width of the Gaussian at fixed time, represented by equation (8), likewise gives an estimate of D_{app}. The width at the point where the Gaussian reaches 1/e of its maximum value is given by x_o, where

$$e^{-1} = \exp\left(-\frac{x_0^2}{4D_{app}t}\right) \quad (10)$$

$$x_0^2 = 4D_{app}t \quad (11)$$

such that D_{app} is the slope of a plot of x_o^2 versus 4t.

The analysis given in this paper will concentrate on measuring D_{app} (equation 1) from such plots as a function of the Ca^{2+}-binding ratio of the indicator dye fura-2. It should be pointed out, though, that due to the analogy between equation (4) and the cable equation (see Zador and Koch, 1994), D_{app} can also be determined from a length constant λ and the intrinsic time constant τ (equation 7) according to

$$D_{app} = \sqrt{\lambda^2/\tau} \quad (12)$$

where

$$\lambda^2 = a(D_{ca} + \sum_i D_{m,i}\kappa_{m,i})/2P_m \quad (13)$$

If, for simplicity, we consider one endogenous mobile buffer species with diffusion coefficient and Ca^{2+}-binding ratio D_m and κ_m, respectively, and one fixed buffer species with κ_s, and in addition the indicator dye with D_b and κ_b , we obtain from equation (1):

$$D_{app} = (D_{Ca} + D_m\kappa_m + D_b\kappa_b)/(1 + \kappa_s + \kappa_m + \kappa_b) \quad (14)$$

The equation can be further simplified by introducing lumped parameters for the endogenous buffers:

$$\kappa_e = \kappa_s + \kappa_m \quad (15)$$

$$D_e = D_m \frac{\kappa_m}{\kappa_s + \kappa_m} \quad (16)$$

which yields

$$D_{app} = (D_{Ca} + D_e\kappa_e + D_b\kappa_b)/(1 + \kappa_e + \kappa_b) \quad (17)$$

A plot of D_{app} versus κb (defined in analogy to equation 2) has D_b as its asymptotic value at high κ_b, and a y-axis intercept of $(D_{Ca} + D_e\kappa_e)/(1 + \kappa_e)$. A nonlinear least-square fit will provide the values D_e and κ_e individually. D_b can be obtained independently by analyzing the diffusion of fura-2 following a short fura-2 injection in analogy to equation 11, as shown below.

Experimental Determination of the Apparent Calcium Diffusion Coefficient as a Function of κ_b

The procedure that we used to measure the apparent Ca^{2+} diffusion coefficient (D_{app}) in a cylindrical axon is illustrated by Figure 1. For the experiments, we first pressure injected fura-2 pentapotassium into the cell body of a cultured metacerebral neuron. As soon as the fura-2 concentration reached a desirable value, the fura-2 injecting micropipette was pulled out, thereby preventing any further increase in the fura-2 concentration during the experiment. Sufficient time was then allowed for the concentration of the indicator dye to equilibrate throughout the neuron (~10 min). The final concentration of fura-2 in the axonal segment was estimated as described in the Experimental Procedures. Fura-2 leakage from the neuron during the experiments (~20 min) was negligible.

We next inserted a calcium-containing micropipette into the axon. After the acquisition of control fura-2 ratio images (Figure 1A, control), Ca^{2+} was briefly (0.2–0.4 s) pressure injected into the axon while acquiring ratio images at a rate of 1 image /1.8 s, for a duration of 40–60 s. Injection strength was adjusted, such that peak $[Ca^{2+}]$ did not exceed 600 nM for the second and later images. The radial calcium concentration gradient formed in the axoplasm at the end of the injection equilibrated within 1 s (Figure 1A; 0 s and 1.8 s). In contrast to that, the diffusion along the longitudinal axis of the axon dissipated at a significantly slower rate (~15–20 s). Thus, the experimental conditions approached the theoretical assumptions, since only longitudinal calcium concentration gradients existed, and peak [Ca] was smaller than the dissociation constant of fura-2 over most images.

After a rest period of 3–5 min, which allowed complete recovery of the $[Ca^{2+}]_i$ gradient, the procedure of intracellular Ca^{2+} injection was repeated up to three times. Thereafter, the calcium-containing micropipette was withdrawn from the axon, and the fura-2-containing micropipette was reinserted into the cell body.

Additional amounts of fura-2 were injected into the soma to elevate the cytoplasmic fura-2 concentration. We then pulled out the fura-2-containing micropipette, time was allowed for fura-2 equilibration, and the procedure of calcium injection and imaging of its spatiotemporal distribution pattern was repeated. In some of the experiments, this sequence of taking images could be performed at three consecutively increasing fura-2 concentrations.

The $[Ca^{2+}]_i$ profiles along the longitudinal axis of the axon at specific points in time were obtained from the fura-2 ratio images (Figure 2A). The $[Ca^{2+}]_i$ profile at each point in time was fitted by a Gaussian (Figure 2A: dotted lines), and D_{app} at a given fura-2 concentration was estimated from the relation of the width parameter as a function of time, as described in the theoretical section (equations 10 and 11; Figure 2B). The minimal fura-2 concentration that we used in these experiments was 25 μM, as concentrations lower than that did not permit reliable imaging of the signal. The experimental points describing the relationships between D_{app} and κ_b are plotted in the graph of Figure 3. At higher concentrations of fura-2, values agreed with those previously determined in Aplysia nerve cell bodies by Nasi and Tillotson (1985) using arsenazo III. However, as shown below, these are strongly influenced by the presence of the indicator dye, such that an extrapolation to zero dye

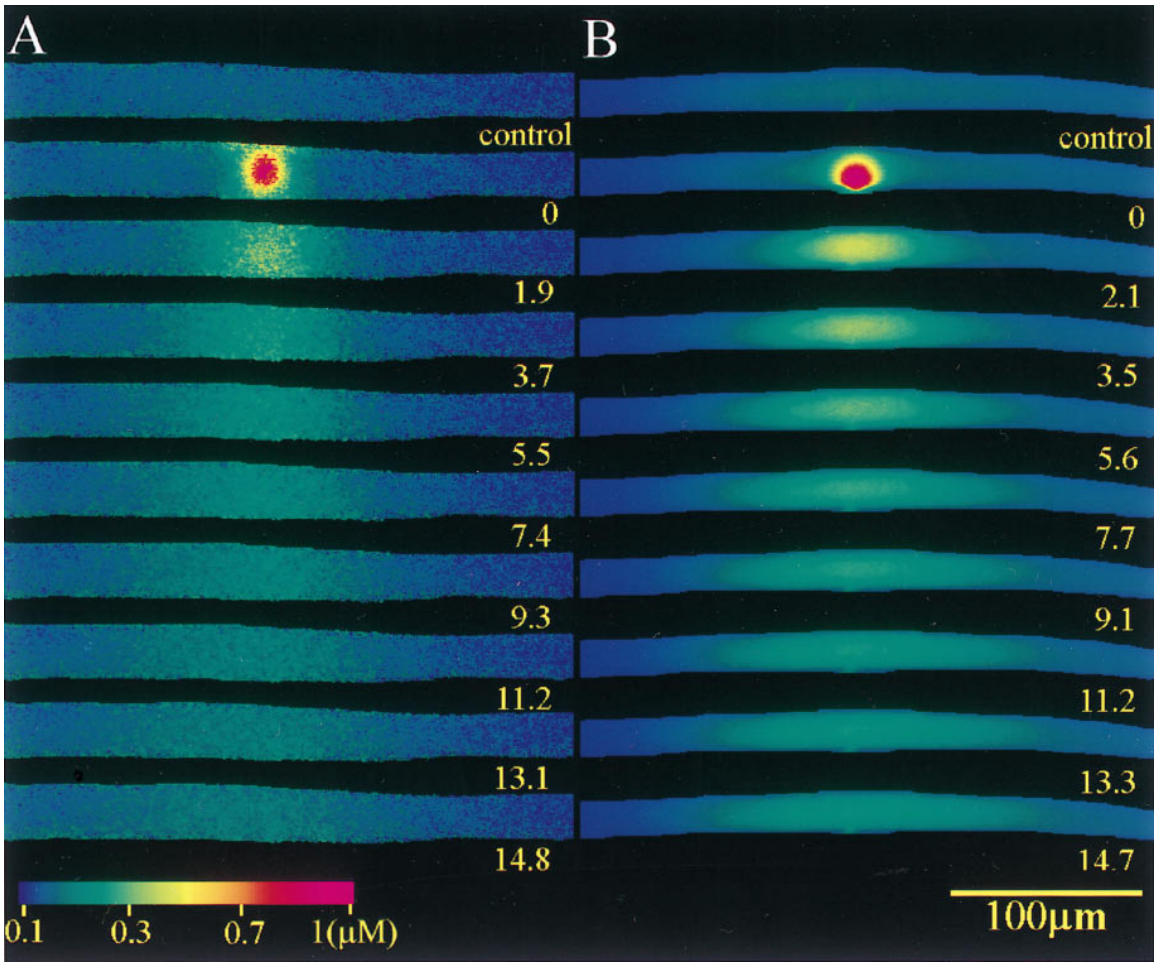

Figure 1. Pseudocolor Images of the Spatiotemporal Distribution Pattern of Calcium Ions (A) and Fura-2 (B)

(A) Fura-2 ratio images of the free intracellular Ca^{2+} following a brief intracellular microinjection of Ca^{2+}. A cultured metacerebral neuron was loaded by intracellular injection of fura-2 pentapotassium to reach a final concentration of 130 μM. The Ca^{2+} solution was pressure injected into the axon by a brief (0.2–0.4 s) pulse from a micropipette containing 100 μM Ca^{2+}. Images were used to create the spatiotemporal concentration profiles shown in Figure 2. Control–before calcium injection, 0' defines the injection time. Calibration of $[Ca^{2+}]_i$ is given in micromolar. Time is given in seconds from injection.

(B) Spatiotemporal distribution pattern of fura-2. The spatiotemporal distribution pattern of fura-2 was imaged following a brief (0.1–0.2 s) pressure injection pulse of the indicator into the axon. The images were grabbed at 360 nm excitation wavelength and used to calculate the diffusion coefficient of the calcium indicator (see Figure 2).

concentration is necessary for estimating the endogenous properties of the cytoplasm.

Estimation of the Fura-2 Diffusion Coefficient along the Axon

A second parameter necessary for the analysis is the diffusion coefficient of the exogenous buffer fura-2. To obtain this parameter experimentally, we used procedures similar to those described above for the measurements of D_{app}. Briefly, fura-2 pentapotassium was pressure injected (0.1–0.2 s) into an axon while continuously imaging its spatiotemporal distribution pattern at an excitation wavelength of 360 or 380 nm (no significant differences were observed while comparing the results obtained by the two excitation wavelengths). The images of the fura-2 concentration gradients at specific points in time (Figure 1B) were subtracted from an image of the fluorescence observed prior to the injection of the dye in order to set the baseline to zero. The resulting image was translated to a graph form (Figure 2C), and the relation of x^2/time*4 was obtained from Gaussian functions fitted to the concentration gradients of subsequent images (Figure 2D). The fura-2 diffusion coefficient (D_b) was found to be 102.5 ± 15.4 $\mu m^2/s$ (mean ± S.D.). No correlation between D_b and concentration of fura-2 was observed between 10 and 250 μM.

Estimation of the Average Diffusion Coefficient of the Endogenous Buffers and Their Ca^{2+}-Binding Ratio

To estimate the average diffusion coefficient of the endogenous buffers D_e and their Ca^{2+}-buffering ratio κ_e, we plotted the experimental values obtained for D_{app} as a function of κ_b (Figure 3). The fura-2 buffering ratio was calculated by $\kappa_b = ([B_T]/K_D)*(1/(1 + ([Ca^{2+}]_i/K_D)^2)$. $[B_T]$, the total concentration of fura-2, was obtained as described in Experimental Procedures, and K_D was set to 760 nM (Grynkiewicz et al., 1985; Ziv and Spira, 1993,

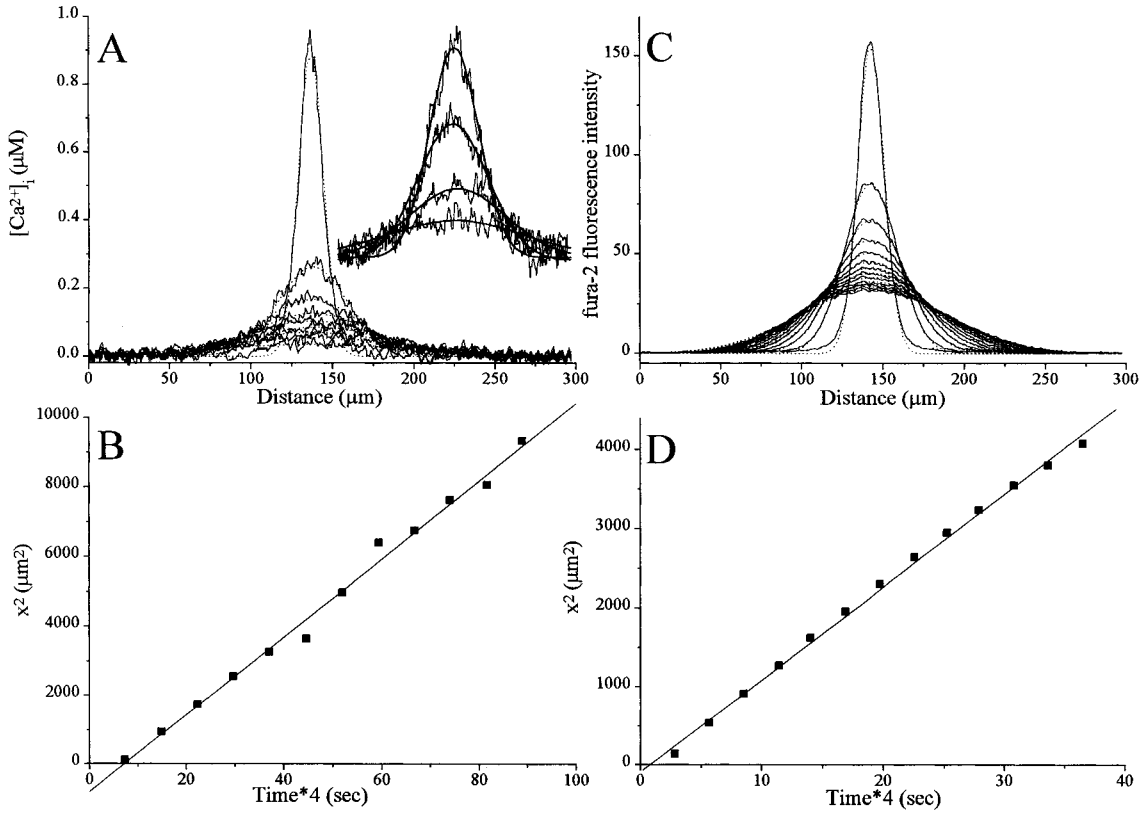

Figure 2. Determination of the Diffusion Coefficients of Calcium and Fura-2 along a Cylindrical Axonal Segment of the Metacerebral Neuron

The apparent diffusion coefficients of Ca^{2+} (D_{app}) and fura-2 (D_b), were estimated from experiments of the type illustrated by Figures 1A and 1B. The calcium concentration profiles (A) or the indicator concentration profiles (C) at different time intervals after a brief intracellular injection were plotted (full lines). A baseline value was subtracted from each curve, such that profiles approached zero at large distance from the injection site. These profiles were fitted by Gaussians (dotted lines), and the square of the width parameter of the Gaussian was plotted as a function of the time after injection. The first points in (B) and (D) correspond to the first images after the injection (highest profiles in parts [A] and [C]) and all subsequent images in (A) and (C) are represented by consecutive points in (B) and (D). The second, third, fifth, and seventh profiles are displayed, in addition, as enlarged inserts in (A) for clarity. The slopes of the plots in (B) and (D) are proportional to D_{app} and D_b, respectively. The value of the apparent diffusion coefficient of Ca^{2+} in this experiment was 112 $\mu m^2/s$ (B) and for fura-2 108.3 $\mu m^2/s$ (D).

1995). The experimental points of the graph of Figure 3 were fitted by the curve described by equation 17. For the calculation, we used $D_b = 102$ $\mu m^2/s$, as obtained in our experiments (Figure 2), and $D_{Ca} = 223$ $\mu m^2/s$ (Allbritton et al., 1992). Combinations of D_e values in the range of 1–30 $\mu m^2/s$ and endogenous calcium binding ratio values (κ_e) in the range of 10–60 were used to fit the theoretical curve to the experimental points. A reasonable fit with $D_e = 14$ $\mu m^2/s$ *and* $\kappa_e = 50$ is shown in Figure 3 (solid line; see figure legend).

To estimate the value of the calcium diffusion coefficient in the unperturbed axon (D_{axo}), the y-axis intercept of a fit to the data in Figure 3 must be obtained. Unfortunately, the back-extrapolation to $\kappa_b = 0$ cannot be performed very accurately since it is not possible to obtain reliable data at low enough dye concentrations. However, inspection of Figure 3 shows that 20 $\mu m^2/s$ can be considered as an upper bound to D_{axo} since this value should not be higher than the linear back-extrapolation of the lowest data points. Likewise, $\kappa_e = 60$ should be an upper bound to the endogenous Ca^{2+}-binding ratio. D_{axo} is significantly lower than the diffusion coefficients of known mobile Ca^{2+}-binding proteins such as Calbindin (Mw 28 kDa) and Calmodulin (Mw 20 kDa), which possess aqueous diffusion coefficients >100 $\mu m^2/s$. This shows that a dominant fraction of the endogenous calcium buffers is either stationary or has very high molecular weight, as in adrenal chromaffin cells and in pyramidal neurons (Neher and Augustine, 1992; Zhou and Neher, 1993; Neher, 1995; Helmchen et al., 1996). The value, however, is close to the values reported by Allbritton et al. (1992) for Ca^{2+} diffusion at basal calcium concentrations in untreated intact cytoplasmic extracts of Xenopus oocytes ($\sim$13 $\mu m^2/s$), to values reported by Al-Baldawi and Abercrombie (1995b) for intact Myxicola axoplasm ($\sim$10 $\mu m^2/s$), and to those reported by Kushmerick and Podolsky (1969) for frog muscles ($\sim$14 $\mu m^2/s$). Unlike in the case of other experimental systems, in which concern was raised that mobile buffers were washed away, the procedures that we used assured that no washout of endogenous mobile buffers took place. In addition to previous estimates, our method provides limits to mobility and Ca^{2+}-binding ratio of buffers. This is important for the considerations below since this knowledge is required to predict changes in D_{app} upon addition of dye or upon expression of Ca^{2+}-binding proteins.

Our value for the diffusion coefficient of fura-2 is more

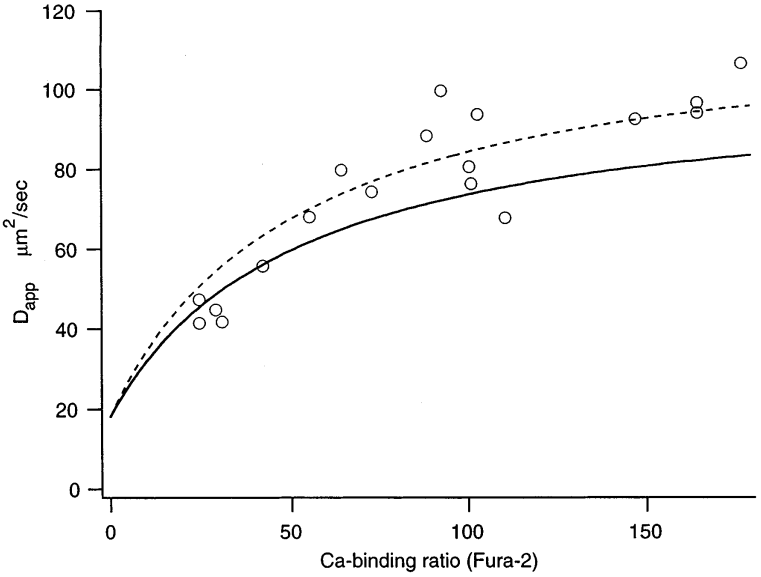

Figure 3. The Apparent Calcium Diffusion Coefficient (D_{app}) along an Axonal Segment as a Function of the Calcium-Binding Ratio of Fura-2 (κ_b)

Open circles are experimental values. The continuous line represents a theoretical curve according to equation 17 with $\kappa_e = 50$ and $D_e = 14$ μm^2/s. This results in an extrapolated value at $\kappa_b = 0$ of $D_{app} = 19$ μm^2/s. The fit is not perfect because it was forced to $D_{fura} = 102$ μm^2/s, which was determined independently. A slightly higher value ($D_{fura} = 118$ μm^2/s, which is the mean + 1 S.D.) gives a much better fit (broken line).

than twice that found in skeletal muscle (Timmermann and Ashley, 1986), but only about half of that given by Strautmann et al. (1990) for the sea lamprey axons. It is close to one fourth of that found for fura-2 in aqueous solution (Timmermann and Ashley, 1986), which is a 2-fold reduction in addition to the 2-fold reduction of diffusion coefficients that is generally found for small molecules in cytosol (Kushmerick and Podolsky, 1969). This indicates that the dye is bound to cytoplasmic structures but not as strongly as it was reported for muscle.

Our method of estimating D_{app} can readily be adapted to other neuronal preparations, where [Ca^{2+}] can be focally and briefly elevated—such as by microinjection or local photolysis of caged compounds. It is conceivable that somata of neurons are loaded with a mixture of dextran-coupled dye and caged Ca^{2+}. Upon spatial equilibration, cylindrical portions of an axon or an apical dendrite might then be stimulated by a focused spot of ultraviolet light, and the ensuing Ca^{2+} signal analyzed according to the procedures described here. Such a sequence could be repeated many times since only a minute fraction of caged Ca^{2+} would be used up during a pulse of local photolysis, and, thus, activity-dependent changes in Ca^{2+} buffering might be revealed.

At present, we have no way to assess the contributions of the various mobile and stationary endogenous buffers to D_{app} because their properties and concentrations in our cells are not known. Nevertheless, if we use the upper bounds to D_{axo} and κ_e discussed above (which implies an upper bound for $D_e = 16$ μm^2/s), we can explore the impact of changes in expression of defined Ca^{2+}-binding proteins on Ca^{2+} signaling. This question is important because proteins like Calmodulin, Calbindins, Parvalbumin, and Calretinine are expressed at widely varying degrees in neurons of the central nervous system (reviewed by Heizmann and Braun, 1995). Several of these proteins are developmentally regulated (Fierro and Llano, 1996; Lohmann and Friauf, 1996) or are regulated in an activity-dependent way (Lowenstein et al., 1991; Heizmann and Braun, 1995). The answer to this question is that, given the low background of mobile buffers, as we find in Aplysia nerve axons, expression of small amounts of typical Ca^{2+}-binding proteins will have profound effects on Ca^{2+} signal amplitude and kinetics. However, such changes will be concealed in the Ca^{2+} measurement due to the buffering effects of Ca^{2+} indicator dyes. These assertions are substantiated in Table 1, where both relative signal amplitude and the relative D_{app} are calculated according to equation 17 for several cases in which different amounts of either a Ca^{2+}-binding protein, or a dye, or a combination of both is added onto the buffer background specified above. It is seen that, for example, addition of 75 μM parvalbumin changes D_{app} almost 3-fold, while addition of 100 μM fura-2 (a low concentration of indicator dye for typical imaging studies) changes D_{app} more. Therefore, addition of both parvalbumin and fura-2 gives a result not much different from that of fura-2 alone. The situation is also quite critical when initial amplitudes of Ca^{2+} signals are calculated. Addition of the protein would change the signal amplitude about 7-fold; this change reduces to 3-fold when dye is present (comparing the case of 100 μM fura-2 with that of 100 μM fura-2 plus 75 μM parvalbumin). At high protein concentration, however (e.g., 1 mM, which was found in axons of cerebellar Purkinje cells), the influence of the dye is not very large. Table 1 also shows that a low affinity dye (Ca-green5N) attenuates the signals much less. However, it appreciably changes D_{app}.

The present study suggests that in the metacerebral neuron of Aplysia the endogenous Ca^{2+}-buffers are mainly stationary and the Ca^{2+}-binding ratio is low (20–60). Earlier studies estimated the Ca^{2+}-binding ratio of the majority of cell types to be in the range of 50–150 (reviewed by Neher, 1995). This includes previous estimates of Ca^{2+}-binding capacity in Aplysia neuronal cell bodies: Smith and Zucker (1980) found that 1% of the calcium entering a cell is reported by Arzenazo III, and Ahmed and Connor (1988) calculated a Ca^{2+} buffer capacity of 45.2 μM/ΔpCa, which is compatible with κ =

Table 1. The Impact of Exogenous and Endogenous Buffer on Ca^{2+} Signals

Cytosolic constituents concentration in μM	Signal amplitude %	Relative D_{app} %
Endogenous buffers	100	100
Plus 100 fura-2	37	367
Plus 200 Ca-green5N	77	196
Plus 75 parvalbumin	15	277
Plus 75 parvalbumin, plus 100 fura-2	12	328
Plus 1000 parvalbumin	1.4	306
Plus 1000 parvalbumin, plus 100 fura-2	1.3	309
Plus 75 parvalbumin, plus 200 Ca-green	15	288

A buffer background compatible with the one observed in this study in Aplysia axons is assumed (κ_e = 60; D_e = 16 μm²/s; D_{Ca} = 223 μm²/s). This results in D_{cyto} = 19 μm²/s, which was set to 100% in the table. It is calculated by how much the apparent diffusion coefficient D_{app} (equation 1) and the amplitude of a Ca^{2+}-signal (assumed to be inversely proportional to the sum of all κ−values) are expected to change if either an indicator dye or a given Ca^{2+}-binding protein is added. Diffusion coefficients for indicator dyes were assumed to be 102 μm²/s, the value we found for fura-2. Diffusion coefficients for proteins were assumed to be 60 μm²/s, half of that reported for parvalbumin in aqueous solution (Konosu et al., 1965). Resting [Ca^{2+}], which is required for calculation of κ−values, was assumed to be 100 nM. The dissociation constant for fura-2 was assumed to be 760 nM (a value close to the mean of those found for in vivo calibrations in several cell types), that of Ca-green 5N as 11 μM (Yao and Parker, 1994). For Ca^{2+} binding to Parvalbumin, two equivalent binding sites with a K_D = 200 nM, taking into account the presence of free Mg^{2+} (Benzonana et al., 1972), were assumed. The concentrations of the proteins were chosen as those found in axons and dendrites, respectively, in cerebellar Purkinje and basket cells (Kosaka et al., 1993).

65 at 300 nM [Ca^{2+}]. However, there are examples for higher and more specific Ca^{2+} buffers in neurons: Roberts (1993) suggested that frog saccular hair cells contain millimolar concentration of mobile endogenous buffer with an estimated diffusion coefficient similar to that of EGTA and BAPTA. Likewise, Kosaka et al. (1993) detected 1 m equivalent/l or more of Ca^{2+}-binding sites (parvalbumin) in axons of cerebellar Purkinje cells, and Fierro and Llano (1996) found the Ca^{2+}-binding ratio of endogeneous buffers in these cells to change from a value of ≈900 at postnatal day 6 to ≈2000 in 15-day-old rats. A similar situation may hold for many other cell types in the central nervous system, which stain heavily for antibodies against various Ca^{2+}-binding proteins (Oberholtzer et al., 1988; Hermann et al., 1991; Baimbridge et al., 1992). The analysis presented shows that D_{cyto} should increase strongly when a neuron changes from the situation characterized by a low background of largely immobile Ca^{2+} buffers to the latter one. Such changes are likely to occur in vivo since numerous examples of changes in expression of Ca^{2+}-binding proteins, either developmentally regulated or regulated in an activity-dependent manner, have been documented (reviewed by Heizmann and Braun, 1995). While it has been amply appreciated in the literature that an increase in buffering power with increasing expression of Ca^{2+}-binding proteins may have an important role in limiting the amplitude of the Ca^{2+} signal and in protecting against excitotoxicity (Mattson et al., 1991), the effect of changes in D_{cyto} may not be so conspicious, even more so since they would not show up in standard Ca^{2+}-imaging experiments. As shown above, expression of 75 μM parvalbumin would lead to a large change of Ca^{2+} dynamics, if this happens against the low background of buffers, as we find for Aplysia axons. In the presence of dye, however, the change is very small.

Increased D_{cyto} will primarily provide for accelerated redistribution of calcium on the length of a scale of 1 to several micrometers. This implies reduction of the signal at its source and a larger range of action. According to the simplified analysis of Zador and Koch (1994), the latter effect can be conveniently described by a prolonged length constant (see also equation 12). In addition, extra mobile buffer will have an effect on the submicroscopic scale by restricting the so-called 'micro'-or nanodomains of Ca^{2+} elevation in the immediate vicinity of Ca^{2+} channels (Kasai, 1993; Roberts, 1993). A full understanding of all of the factors that influence Ca^{2+} signaling will therefore require more detailed studies and less invasive techniques for Ca^{2+} imaging. An important step toward this goal would be the use of less mobile Ca^{2+} indicator dyes, such as the dextran-coupled varieties.

Experimental Procedures

Cell Culture

Juvenile specimens of Aplysia californica were used. The culturing procedures were carried out as previously described (Ziv and Spira, 1993, 1995; Spira et al., 1993). Briefly, cerebral ganglia were isolated, and incubated for 1.5–2.5 hr in 1% protease (Sigma type IX) at 35°C. The ganglia were then desheathed, the cell body of the metacerebral neurons (Kandel, 1976) with their long axons were pulled out with sharp micropipettes and placed on poly-L-lysine (Sigma) coated glass-bottom culture dishes. The culture medium consisted of equal parts of filtered hemolymph from Aplysia faciata collected along the Mediterranean coast, and L-15 supplemented for marine species (Ziv and Spira, 1993, 1995; Spira et al., 1993).

Loading of Calcium-Sensitive Indicators

The cell body was impaled by a 5–8 MΩ microelectrode filled with 2M KCl and 10 mM fura-2 as a potassium salt (Molecular Probes). The indicator was loaded into the neurons by pressure injection. A neuron was loaded to a final desirable indicator concentration of 25–175 μM. The final intracellular fura-2 concentration was estimated by comparing the indicator fluorescence of the axon at the 380 nm or 360 nm excitation wavelengths with the fluorescence measured at the appropriate wavelength in glass micropipettes pulled to a diameter similar to that of the axon and containing known indicator concentrations. For the calibration measurements, the indicator was dissolved in a solution containing 250 mM KCl, 20 mM HEPES, and 7 mM EGTA (ethyleneglycol-bis-(b-aminoethyl ether) N',N',N',N'- tetraacetic acid) at pH 7.4.

$[Ca^{2+}]_i$ Imaging

Essentially, we used the procedure developed by Grynkiewicz et al. (1985), as detailed by Ziv and Spira (1993, 1995). Briefly, fluorescence images of the neurons loaded with fura-2 were taken by online averaging of eight video frames at 340 ± 5 and 380 ± 5 nm excitation wavelengths. As the axons' autofluorescence was negligible compared with the fluorescence intensity of the Ca^{2+} indicators, background images at excitation wavelengths of 340 and 380 nm were obtained from regions adjacent to the neuron to be tested. The background images were subtracted from the averaged images obtained at 340 and 380 nm. Ratio images of the fluorescent intensities were obtained by dividing each pixel in the 340 nm fluorescence image by the corresponding pixel in the 380 nm image.

The fluorescent microscope system consisted of a Zeiss Axiovert microscope equipped with a 75 W Xenon arc lamp, a Zeiss 40 ×

0.75 NA Plan-Neofluar objective, 340 ± 5 nm and 380 ± 5 nm band pass excitation filters mounted in a computer-controlled Lambda filter changer, a dichroic mirror with a cut-off threshold of 395 nm, and a 510 ± 10 nm band pass emission filter. To prevent unnecessary exposure of the neurons to the excitation light, a computer-controlled electronic shutter (Uniblitz) was placed in the light path. The images were collected with an intensified CCD video camera (Hamamatsu), digitized at 512 × 512 pixels with a PC-hosted frame grabber (Imaging Technologies). Images were stored as computer files and processed using a software package written in our laboratory.

Calibration of the Fura-2 Signals

The fura-2 ratio values were converted to free intracellular Ca^{2+} concentrations by means of a calibration curve (Grynkiewicz et al., 1985) as previously described (Ziv and Spira, 1993). Briefly, a series of buffered solutions at defined free Ca^{2+} concentrations were prepared, and 5 μl samples containing 10 μM fura-2 pentapotassium were placed on a cover slide. Fluorescence values and ratios for each solution were calculated. A theoretical curve was produced according to the equation of Grynkiewicz et al. (1985). The following values were used: $R_{min} = 0.218$; $R_{max} = 8.53$; and $Sf2/Sb2 = 12.9$. As the exact values of these parameters tended to change with time, the system was recalibrated routinely. For the generation of the calculated calibration curve, we assumed a dissociation constant of fura-2 and Ca^{2+} of 760 nM according to Grynkiewicz et al. (1985).

Determination of the Intracellular Diffusion Coefficient of Fura-2

To determine the diffusion coefficient of fura-2 in the axonal segment, we imaged the spatiotemporal distribution pattern of fura-2 microinjected into the axon. Because of the cylindrical structure of the axon and the relatively rapid equilibration of the fura-2 concentration across the radial axis of the axon, it is possible to reduce the model of the diffusion of a dye injected for a brief duration into one point along the axon to a model of one-dimensional diffusion from a disc source. This model can be described by the function:

$$y(x,t) = A_o \frac{\exp(-x^2/(4D_b t))}{\sqrt{4\pi D_b t}}$$

where t is the time from injection, x is the distance from the point of injection, $y(x,t)$ is the fluorescent signal of the dye at location x and time t, A_o is a constant amplitude factor, and D_b is the diffusion coefficient of the dye.

By fitting Gaussians to plots of the observed fluorescent intensity along an injected axon taken at fixed time intervals from the injection onward and by extracting the x parameter, it is possible to plot x^2 as a function of $4*t$ and calculate D_b from the slope in analogy to the calculation of D_{Ca} (equation 11).

Acknowledgments

This study was supported by a grant from the German Israel Foundation for Scientific Research and Development (No. I-392—216.01/94) to professor Spira, Dr. Müller, and professor Neher. E. N. was also supported by a grant from the Behrens Weise Stiftung. M. E. S. is the Levi DeViali professor in neurobiology.

Received September 12, 1996; revised January 31, 1997.

References

Ahmed, Z., and Connor, J.A. (1988). Calcium regulation by and buffer capacity of molluscan neurons during calcium transients. Cell Calcium *9*, 57–69.

Al-baldawi, N.F., and Abercrombie, R.F. (1995a). Cytoplasmic calcium buffer capacity determined with Nitr-5 and DM-nitrophen. Cell Calcium *17*, 409–421.

Al-baldawi, N.F., and Abercrombie, R.F. (1995b). Calcium diffusion coefficient in Myxicola axoplasm. Cell Calcium *17*, 422–430.

Allbritton, N.L., Meyer, T., and Stryer, L. (1992). Range of messenger action of calcium ion and inositol 1,4,5-trisphosphate. Science *258*, 1812–1815.

Baimbridge, K.G., Celio, M.R., and Rogers, J.H. (1992). Calcium-binding proteins in the nervous system. Trends Neurosci. *15*, 303–308.

Benzonana, G., Capony, J.-P., and Pechere, J.F. (1972). The binding of calcium to muscular parvalbumins. Biochim. Biophys. Acta *278*, 110–116.

Falke, J.J., Drake, S.K., Hazard, A.L., and Peersen, O.B. (1994). Molecular tuning of ion binding to calcium signaling proteins. Q. Rev. Biophys. *27*, 219–290.

Fields, R.D., and Nelson, P.G. (1994). Resonant activation of calcium signal transduction in neurons. J. Neurobiol. *25*, 281–293.

Fierro, L., and Llano, I. (1996). High endogeneous calcium buffering in Purkinje cells from rat cellular slices. J. Physiol. *496*, 617–625.

Grynkiewicz, G., Poenie, M., and Tsien, R.Y. (1985). A new generation of Ca^{2+} indicators with greatly improved fluorescence properties. J. Biol. Chem. *260*, 3440–3450.

Heizmann, C.W., and Braun, K. (1995). Calcium regulation by calcium-binding proteins in neurodegenerative disorders. (Heidelberg: Springer Verlag).

Helmchen, F., Imoto, K., and Sakmann, B. (1996). Ca^{2+} buffering and action potential-evoked Ca^{2+} signaling in dendrites of pyramidal neurons. Biophys. J. *70*, 1069–1081.

Hermann, A., Pauls, T.L., and Heizmann, C.W. (1991). Calcium-binding proteins in *Aplysia* neurons. Cell. Mol. Neurobiol. *11*, 371–386.

Hodgkin, A.L., and Keynes, R.D. (1957). Movement of labelled calcium in squid giant axons. J. Physiol. *138*, 253–281.

Jaffe, D.B., Johnston, D., Lasser-Ross, N., Lisman, J.E., Miyakawa, H., and Ross, W.N. (1992). The spread of Na+ spikes determines the pattern of dendritic Ca^{2+} entry into hippocampal neurons. Nature *357*, 244–246.

Kasai, H. (1993). Cytosolic Ca^{2+} gradients, Ca^{2+} binding proteins and synaptic plasticity. Neurosci. Res. *16*, 1–7.

Konosu, S., Hamoir, G., and Pechère, J.-F. (1965). Carp myogen of white and red muscles: properties and amino acid composition of the main low molecular-weight components of white muscle. Biochem. J. *96*, 98–112.

Kosaka, T., Kosaka, K., Nakayama, T., Hunziker, W., and Heizmann, C.W. (1993). Axons and axon terminals of cerebellar Purkinje cells and basket cells have higher levels of parvalbumin immunoreactivity than somata and dendrites: quantitative analysis by immunogold labeling. Exp. Brain Res. *93*, 483–491.

Kushmerick, M.J., and Podolsky, R.J. (1969). Ionic mobility in muscle cells. Science *166*, 1297–1298.

Lohmann, C., and Friauf, E. (1996). Distribution of the calcium-binding proteins parvalbumin and calretinin in the auditory brainstem of adult and developing rats. J. Comp. Neurol. *367*, 90–109.

Lowenstein, D.H., Miles, M.F., Hatam, F., and McCable, J. (1991). Up regulation of Calbindin-D28K mRNA in the rat hippocampus following focal stimulation of the perforant path. Neuron *6*, 627–633.

Mattson, M.P., Rychlik, B., Chu, C., and Christakos, S. (1991). Evidence for calcium-reducing and excito-protective roles for the calcium-binding protein calbindin-D_{28k} in cultures hippocampal neurons. Neuron *6*, 41–51.

Miller, R.J. (1991). The control of neuronal Ca^{2+} homeostasis. Prog. Neurobiol. *37*, 255–285.

Nasi, E., and Tillotson, D. (1985). The rate of diffusion of Ca^{2+} and Ba^{2+} in a nerve cell body. Biophys. J. *47*, 735–738.

Neher, E. (1995). The use of fura-2 for estimating Ca buffers and Ca fluxes. Neuropharmacology *34*, 1423–1142.

Neher, E., and Augustine, G.J. (1992). Calcium gradients and buffers in bovine chromaffin cells. J. Physiol. (Lond.) *450*, 273–301.

Nowycky, M.C., and Pinter, M.J. (1993). Time course of calcium and calcium-bound buffers following calcium influx in a model cell. Biophys. J. *64*, 77–91.

Oberholtzer, H.C., Buettger, C., Summers, M.C., and Matschinsky,

F.M. (1988). The 28-kDa calbindin-D is a major calcium-binding protein in the basilar papilla of the chick. Proc. Natl. Acad. Sci. USA *85*, 3387–3390.

Roberts, W.M. (1993). Spatial calcium buffering in saccular hair cells. Nature *363*, 74–76.

Sala, F., and Hernandez-Cruz, A. (1990). Calcium diffusion modeling in spherical neuron. Relevance of buffering properties. Biophys. J. *57*, 313–324.

Smith, S.J., and Zucker, R.S. (1980). Aequorin response facilitation and intracellular calcium accumulation in molluscan neurones. J. Physiol. *300*, 167–196.

Spira, M.E., Benbassat, D., and Dormann, A. (1993). Resealing of the proximal and distal cut ends of transected axons: electrophysiological and ultrastructural analysis. J. Neurobiol. *24*, 300–316.

Spruston, N., Schiller, Y., Stuart, G., and Sakmann, B. (1995). Activity-dependent action potential invasion and calcium influx into hippocampal CA1 dendrites. Science *268*, 297–300.

Strautmann, A.F., Cork, R.J., and Robinson, K.R. (1990). The distribution of free calcium in transected spinal axons and its modulation by applied electrical fields. J. Neurosci. *10*, 3564–3575.

Timmermann, M.P., and Ashley, C.C. (1986). Fura-2 diffusion and its use as an indicator of transient free calcium changes in single striated muscle cells. FEBS Lett. *209*, 1–8.

Wagner, J., and Keizer, J. (1994). Effects of rapid buffers on Ca^{2+} diffusion and Ca^{2+} oscillations. Biophys. J. *67*, 447–456.

Yao, Y., and Parker, I. (1994). Ca^{2+} influx modulation of temporal and spatial patterns of inositol trisphosphate-mediated Ca^{2+} liberation in *Xenopus* oocytes. J. Physiol. *476*, 17–28.

Zador, A., and Koch, C. (1994). Linearized models of calcium dynamics: formal equivalence to the cable equation. J. Neurosci. *14*, 4705–4715.

Zhou, Z., and Neher, E. (1993). Mobile and immobile calcium buffers in bovine adrenal chromaffin cells. J. Physiol. (Lond.) *469*, 245–273.

Ziv, N.E., and Spira, M.E. (1993). Spatiotemporal distribution of Ca^{2+} following axotomy and throughout the recovery process of cultured *Aplysia* neurons. Eur. J. Neurosci. *5*, 657–668.

Ziv, N.E., and Spira, M.E. (1995). Axotomy induces a transient and localized elevation of the free intracellular calcium concentration to the millimolar range. J. Neurophysiol. *74*, 2625–2637.